ISSN 1070-3632, Russian Journal of General Chemistry, 2015, Vol. 85, No. 9, pp. 2183–2197. © Pleiades Publishing, Ltd., 2015.

Investigation of Derivatized Schiff Base Ligands of 1,2,4-Triazole Amine and Their Oxovanadium(IV) Complexes: Synthesis, Structure, DNA Binding, Alkaline Phosphatase Inhibition, Biological Screening, and Insulin Mimetic Properties[1]

K. S. Munawar[a], S. Ali[a], M. N. Tahir[b], N. Khalid[c], Q. Abbas[d], I. Z. Qureshi[d], and S. Shahzadi[a]

[a] *Department of Chemistry, Quaid-i-Azam University, Islamabad, Pakistan*
e-mail: drsa54@hotmail.com; sairashahzadi@hotmail.com

[b] *Department of Physics, University of Sargodha, Sargodha, Pakistan*

[c] *Chemistry Division, Pakistan Institute of Nuclear Science & Technology, P.O. Nilore, Islamabad, Pakistan*

[d] *Department of Animal Sciences, Quaid-i-Azam University, Islamabad, Pakistan*

Received July 17, 2015

Abstract—A series of novel azomethine precursors were derivatized by the condensation of 4H-1,2,4-triazole-4-amine with salicylaldehyde (**HL[1]**) (saltrz), 2,3-dihydroxybenzaldehyde (**HL[2]**) (dhtrz), 2-hydroxy-1-naphthaldehyde (**HL[3]**) (ndtrz) and 5-chloro-2-hydroxybenzaldehyde (**HL[4]**) (cltrz). Subsequently, oxovanadium(IV) complexes of the type $[VO(saltrz)_2]$ (**1**), $[VO(dhtrz)_2]$ (**2**), $[VO(ndtrz)_2]$ (**3**), and $[VO(cltrz)_2]$ (**4**) were synthesized by the reactions of vanadyl(V) isopropoxide $[VO(OCHMe_2)_3]$ with the ligands **HL[1]**–**HL[4]**. The synthesized compounds were characterized by the melting point method, elemental analysis, FT-IR and ^1H and ^{13}C NMR spectroscopies, the molar susceptibility and conductivity methods, and by the thermogravimetry. Ligands **HL[3]** and **HL[4]** were also characterized by single crystal analysis. The binding modes of SS-DNA with the compounds were confirmed by the hypochromism and red/blue shift of the UV-Vis spectra. The negative DG values of the compound-DNA adducts show that the binding is a spontaneous process. The complexes were found to be persuasive inhibitors of enzyme alkaline phosphatase (ALP). The in vitro screening of the antimicrobial activities of the synthesized compounds revealed significantly enhanced activities of oxovanadium(IV) complexes as compared to their respective ligands. The promising results were obtained in studying the insulin mimetic of the synthesized compounds.

Keywords: 1,2,4-triazole amine derivatives, oxovanadium(IV) complexes, DNA binding, alkaline phosphatase inhibition, antimicrobial activities, hemolysis, insulin mimetic properties

DOI: 10.1134/S1070363215090248

INTRODUCTION

In recent years, coordination chemistry of vanadium has aroused interest of researches, since this compound is involved into several biological processes, is present in organisms such as *Ascidians* and *Amanita* mushrooms, and is a constituent of the cofactors in vanadate-dependent haloperoxidases and vanadium nitrogenase [1–4].

The vanadium compounds exhibit marked hypoglycemic activity and are used as antidiabetic drugs [5–7]. They are also known as prospective inhibitors of various enzymes, such as alkaline phosphatase. Inorganic vanadium compounds, like vanadyl sulfate and vanadate, are poorly diffused through the gastric and intestinal tracts and are more toxic. Therefore, vanadium(IV) compounds are preferred for *in vivo* administration [8, 9]. The nature of organic ligands in vanadyl complexes is related to their pharmaco-

[1] The text was submitted by the authors in English.

kinetics. The catalytic, biological, and medicinal properties of the vanadium complexes have stimulated the scientists to synthesize new more active model vanadium compounds containing O and N donor ligands.

Schiff-base ligands prepared by the condensation of aromatic aldehydes and polyamines are highly promising compounds, as they exhibit higher efficiency for the above mentioned processes. The modification of amino-heterocyclic compounds, such as triazoles, into Schiff bases might result in the formation of polydentate ligands with interesting properties. The derivatives of 1,2,4-triazole are efficient ligands for coordination with vanadium ions [10, 11].

Based on the properties of existing triazoles, a new series of triazole derivatives and their oxovanadium complexes were synthesized and their potency as DNA binders, alkaline phosphatase inhibitors, antimicrobial agents, and especially, insulin mimetics was evaluated.

EXPERIMENTAL

Chemicals and instrumentation. Solvents and reagents were obtained from commercial sources and used without further purification unless otherwise stated. Vanadyl(V) isopropoxide, 4*H*-1,2,4-triazole-4-amine, salicylaldehyde, 2,3-dihydroxybenzaldehyde, 2-hydroxy-1-naphthaldehyde, 5-chloro-2-hydroxybenzaldehyde, *p*-nitrophenyl phosphate hexahydrate (*p*-NPP), diethanolamine and magnesium chloride were purchased from Sigma Aldrich. Sodium salt of Salmon sperm DNA (SS-DNA) was obtained from Acros Organics and used as received. Human serum was used as a source of alkaline phosphatase (ALP). Elemental analysis of the synthesized compounds was carried out on an Elemental Vario EL elemental analyzer. FT-IR spectra in the range of 4000–250 cm^{-1} were obtained on a Thermo Nicolet-6700 FT-IR spectrophotometer. Multinuclear (^1H and ^{13}C) NMR spectra were recorded on a Bruker-400 MHz FT-NMR Spectrometer, using DMSO-d_6 as a solvent [δ ^1H (DMSO) = 2.5 ppm and δ ^{13}C (DMSO) = 39 ppm]. Chemical shifts are given in ppm and coupling constants (*J*), in Hz. The multiplicity of ^1H NMR signals (s = singlet, d = doublet, d.d = doublets of doublet, t = triplet, d.d.d. = doublet of doublet of doublets, and m = multiplet) is indicated with chemical shifts. The absorption spectra were recorded on a Shimadzu 1800 UV-Vis Spectrophotometer. The melting points were determined in capillary tubes using an electrothermal melting point apparatus (gallenkamp). Magnetic moment was determined on a Sherwood magnetic susceptibility balance at ambient temperature (25±2°C) with $Hg[Co(SCN)_4]$ as calibrant. Thermogravimetric analysis was performed with Universal V4.3A TA Instruments. The electrical conductance of 10^{-3} molar solutions in DMSO : H_2O (7 : 3) was recorded on an Elico CM-180 Conductivity Bridg. The X-ray diffraction data wasere collected on a Bruker SMART APEX CCD diffractometer, equipped with a 4 K CCD detector set 60.0 mm from the crystal. The crystals were cooled to 296±1 K using the Bruker KRYOFLEX low temperature device. In measuring the intensity, a MoK_α radiation from a sealed ceramic diffraction tube (SIEMENS) was used. The structure was solved by the Patterson methods (DIRDIF or SIR 2004 program). For the refinement of crystal structure we used a SHELXL-97 program, a modified version of the PLUTO program (preparation of illustrations) and PLATON package [12].

Study of Salmon sperm-DNA binding by the electronic absorption titration. The interaction of ligands and their vanadium complexes with SS-DNA was performed in tris HCl buffer [5 mM of tris (hydroxylmethyl)aminomethane and 50 mM of NaCl at pH 7.2]. A solution of SS-DNA in a buffer gave an absorbance ratio of 1.9 : 1 at 260 and 280 nm, indicating that the SS-DNA was free from protein [13, 14]. The concentration of SS-DNA was measured by using an extinction coefficient of 6600 M^{-1} cm^{-1} at 260 nm and was found to be 2.0×10^{-4} M. The compound was dissolved in DMSO : H_2O (7 : 3) at a concentration of 2 mM. In measurements of the UV-Vis absorption spectra, the SS-DNA concentration was varied, whereas the concentrations of the compound and the reference solution were constant. The compound-SS-DNA solutions were incubated for 30 min at room temperature (25±1°C) before measuring the absorption.

Alkaline phosphatase inhibition . The bioassay of the substrate was prepared by following the reported procedure [15], by mixing four parts of reagent A (diethanolamine pH 9.8, 2 M and magnesium chloride 0.5 mM) and one part of reagent B (*p*-NPP 50 mM). The mixture was incubated for 5 min at 25± 1°C. Into a cuvette, 2 mL of the substrate was poured and 40 μL of human serum having the activity of 165 IU/L was added into it. After 1 min of incubation, the absorbance was measured at 405 nm to confirm enzyme activity. Different aliquots of a 25 mM stock solution of oxovanadium complexes were added to the

above substrate after regular intervals, incubated for 3 min, and the absorbance was then recorded from 1–5 min after each 1 min The average value of these readings was used to calculate the age inhibition (%).

Antimicrobial activities. The fungicidal and bactericidal activities of the synthesized triazole precursors and their respective oxovanadium complexes against various bacteria and fungi were determined by the following methods:

a. Growth medium, culture, and inoculum preparation. The bacterial strains (*Escherichia coli, Bacillus subtilis, Staphylococcus aureus* and *Pasturella multocida*) were cultured overnight at 37°C in nutrient agar. The pure bacterial cultures obtained were stored in the medium in slants and petri plates. For inoculums preparation, 13 g of nutrient broth was suspended in 1 L of distilled water, homogenously mixed, and autoclaved for 15 min at 121°C. Then, 10 μL of pure culture of a bacterial strain was added to 100 mL of freshly prepared nutrient broth medium and shacked (at 140 rpm) for 24 h at 37°C. The prepared inocula were stored at 4°C. The inocula with 1×10^8 spores/mL were used for activity measurement [16].

The fungal strains (*Alternaria alternata, Ganoderma lucidum, Aspergillus niger,* and *Penicillium notatum*) were cultured overnight at 28°C using potato dextrose agar. The pure cultures were maintained in sabouraud dextrose agar (SDA) medium in slants and petri plates, which were presterilized in hot air oven at 180°C for 3 h. These cultured slants were incubated at 28°C for 3–4 days for the multiplication of fungal strains.

b. Measurement of antimicrobial assay by disc diffusion method. Antimicrobial activities were measured by the disc diffusion method [17]. 2.8 g of nutrient agar (for antibacterial activities) or 3.9 g of potato dextrose agar (for antifungal activities) was suspended in 100 mL of distilled water and sterilized by autoclaving at 121°C for 15 min Then, the suspension was thoroughly mixed with 100 μL of inoculum and poured into sterilized petri plates. Finally, a 9-mm filter paper discs soaked with 100 μL of a specific solution were laid flat on the growth medium. The petri plates were then incubated at 37°C for 24 h or at 28°C for 48 h for the bacteria or fungi growth, respectively. Clear zones of the inhibition formed around the discs were measured in millimeters using a zone reader [18, 19].

c. Hemolytic activity. Heparinized fresh human blood (3 mm) was mixed with 15 mL of sterile in a polystyrene screw-captube, centrifuged for 5 min at 850g, the resulting supernatant was poured off and the viscous pellet was washed thriply with 5 mL of chilled (4°C) sterile isotonic phosphate-buffered saline (PBS) having pH 7.4. The washed cells were suspended in 20 mL of chilled PBS and counted on a hemocytometer. The blood cell suspension (maintained on wet ice) was diluted with sterile PBS to 7.068×10^8 cells mL^{-1} for each assay. Aliquots of 20 μL of each sample solutions were placed aseptically into 2.0 mL microfuge tubes. For each assay, 0.1% Triton X-100 was used as positive control (100% lysis) and PBS as negative control (0% lytic). Aliquots of 180 μL diluted blood cell suspension was aseptically placed into each 2 mL tube and mixed gently three times. The tubes were incubated for 35 min at 37°C with agitation (at 80 rpm) and then placed on ice for 5 min., followed by centrifugation for 5 min at 1310 g. Aliquots of 100 μL of supernatant were collected, placed into a sterile microfuge tube (volume 1.5 mL) and then diluted with 900 μL of chilled and sterile PBS. All tubes were maintained on wet ice after dilution. Absorbance at 576 nm was then measured on a Microquant. The experiment was done in triplicate.

Antidiabetic study. *a. Animals and maintenance.* Healthy adult male BALB/c mice (n = 50, average body weight = 35±5 g) were obtained from the "National Institute of Health," Islamabad. Five animals were housed per cage and were given free access to standard rodent diet and water *ad libitum*. Photoperiod was maintained at 12 : 12 hour light/dark cycle.

b. Induction of diabetes. In order to induce diabetes, a single injection of Alloxan monohydrate (Sigma Aldrich, USA) was given intraperitoneally (i.p.) at the dose of 150 mg/kg body weight.The mice with fasting plasma glucose levels > 200 mg/dL were considered diabetic and were selected for further studies.

c. Experimental design. Animals were divided into ten groups, five animals each. They were treated with acute doses (35.9 mg/kg body weight) of compounds $\mathbf{HL^1}$–$\mathbf{HL^4}$ and complexes **1–4**. Positive control groups were treated with a known antidiabetic drug Glibenclamide (10 mg/kg body weight in distilled H_2O) [20]. The treatment groups were as follows:

Control groups. *Group 1:* Negative control (diabetic, only Alloxan pretreated). *Group 2:* Positive control (diabetic, Alloxan pretreated followed by Glibenclamide treatment).

Experimental groups. *Group 3:* Compound **HL^1** treated (diabetic, Alloxan pretreated). *Group 4:* Compound **1** treated (diabetic, Alloxan pretreated). *Group 5:* Compound **HL^2** treated (diabetic, Alloxan pretreated). *Group 6:* Compound **2** treated (diabetic, Alloxan pretreated). *Group 7:* Compound **HL^3** treated (diabetic, Alloxan pretreated). *Group 8:* Compound **3** treated (diabetic, Alloxan pretreated). *Group 9:* Compound **HL^4** treated (diabetic, Alloxan pretreated). *Group 10:* Compound **4** treated (diabetic, Alloxan pretreated).

d. Glucose determination. Blood was collected through a caudal venepuncture using a 26 gauge butterfly cannula. Blood samples were drawn at 0 h (Pre Alloxan), 1 h (Post Alloxan), and at 1–7 h after dosing. Plasma glucose was determined using a dextrostix test strip and an Accu-Check blood glucose meter (Active, Roche Pharma).

e. Determination of total serum cholesterol and triglycerides. Total Serum cholesterol and triglycerides were determined through commercially available kits from Globe Diagnostics (Italy) using Microlab 300 (Germany).

Statistical analysis. The data were analyzed through one-way analysis of variance (ANOVA) using the Statistical Package for Social Sciences (SPSS version, 16.0 Inc. Chicago, Illinois, USA). Post-hoc Tukey-Kramer test and normality test failed; ANOVA on Ranks test was applied. $p < 0.05$ was considered statistically significant difference. Data are presented as line or bar diagrams using the GraphPad Prism 5 (Version 5.01 GraphPad Software Inc., USA).

Syntheses of triazole-based azomethine precursors. *a. Synthesis of (E)-2-[(4H-1,2,4-triazole-4-ylimino)methyl]phenol (**HL^1**).* A dried ethanolic solution of salicylaldehyde (1.25 mL, 1.18 mmol) was added to an ethanolic solution of 4*H*-1,2,4-triazole-4-amine (1 g, 1.18 mmol). The slightly yellow mixture obtained was stirred for 15 min and refluxed for 45 min The resulting pale-yellow solution was cooled to room temperature. The white crystalline solid obtained was filtered off, washed first with ethanol and then with diethyl ether, and, finally, was dried under vacuum. Yield 85%, mp 206°C, IR spectrum, ν, cm^{-1}: 3435 (–OH), 1602 (HC=N), 1299 (C–O), ^{1}H NMR spectrum (DMSO-d_6, 400 MHz, δ, ppm): 10.54 s (–OH), 9.38 s (H^1, H$^{1'}$), 9.19 s (HC=N), 7.02 d.d (H^5, J[^{1}H–^{1}H] = 8.4, 1.6 Hz), 7.44 d.d.d (H^6, J[^{1}H–^{1}H] = 8.4, 1.6 Hz), 6.96 d.d.d (H^7, J[^{1}H–^{1}H] = 8.4, 1.6 Hz), 7.02 d.d (H^8, J[^{1}H–^{1}H] = 8.4, 1.6 Hz); ^{13}C NMR spectrum (DMSO-d_6 101 MHz, δ, ppm): 139.0 (C^1, C$^{1'}$), 156.0 (C^2), 118.0 (C^3), 158.3 (C^4), 116.7 (C^5), 134.2 (C^6), 119.6 (C^7), 127.6 (C^8), Λ_m (DMSO) 2.5 S cm^2 mol^{-1}.

*b. Synthesis of (E)-3-[(4H-1,2,4-triazole-4-ylimino) methyl]benzene-1,2-diol (**HL^2**).* **HL^2** was synthesized by the procedure used for **HL^1.** However, in this case, 2,3-dihydroxybenzaldehyde was used instead of salicylaldehyde. White precipitates were immediately obtained on cooling.Yield 84%, mp 270°C, IR spectrum, ν, cm^{-1} 3453 (–OH), 1610 (HC=N), 1312 (C–O), ^{1}HNMR spectrum (DMSO-d_6 400 MHz, δ, ppm): 10.17 s (–OH), 9.61 s (–OH'), 9.12 s (H^1, H$^{1'}$), 9.10 s (HC=N), 6.93 d.d (H^6, J[^{1}H–^{1}H] = 8.0, 1.6 Hz), 6.73 t (H^7, J[^{1}H–^{1}H] = 8.0 Hz), 7.19 d.d (1H, H^8, J[^{1}H–^{1}H] = 8.0, 1.6 Hz); ^{13}C NMR spectrum (DMSO-d_6 101 MHz, δ, ppm): 138.9 (C^1, C$^{1'}$), 155.5 (C^2), 117.8 (C^3), 147.2 (C^4), 146.0 (C^5), 118.6 (C^6), 118.7 (C^7), 119.4 (C^8), Λ_m (DMSO) 3.8 S cm^2 mol^{-1}.

*c. Synthesis of (E)-1-[(4H-1,2,4-triazole-4-ylimino) methyl]naphthalen-2-ol (**HL^3**).* The procedure of **HL^3** preparation was the same as for **HL^1**. The only difference was that 2-hydroxy-1-naphthaldehyde was used instead of salicylaldehyde. On cooling and evaporation, colorless acicular crystals were collected from the basic liquor after 2 days. Yield 88%, mp 250°C; IR spectrum, ν, cm^{-1} 3442 (–OH), 1618 (HC=N), 1299 (C–O), ^{1}H NMR spectrum (DMSO-d_6 400 MHz, δ, ppm): 11.36 s (–OH), 9.30 s (H^1, H$^{1'}$), 9.66 s (HC=N), 8.06 d (H^5, J[^{1}H–^{1}H] = 8.8 Hz), 7.29 d (H^6, J[^{1}H–^{1}H] = 8.8 Hz), 8.86 d (H^8, J[^{1}H–^{1}H] = 8.8 Hz), 7.45 d.d.d (H^9, J[^{1}H–^{1}H] = 8.4, 6.4, 2.4 Hz), 7.63 d.d.d (H^{10}, J[^{1}H–^{1}H] = 8.4, 6.4, 2.4 Hz), 7.93 d (H^{11}, J[^{1}H–^{1}H] = 8.8 Hz); ^{13}C NMR spectrum (DMSO-d_6 101 MHz, δ, ppm): 138.9 (C^1, C$^{1'}$), 156.5 (C^2), 108.4 (C^3), 159.4 (C^4), 118.4 (C^5), 131.6 (C^6), 128.9 (C^7), 128.3 (C^8), 123.4 (C^9), 128.0 (C^{10}), 123.9 (C^{11}), 135.4 (C^{12}), Λ_m (DMSO) 4.2 S cm^2 mol^{-1}.

*d. Synthesis of (E)-2-[(4H-1,2,4-triazole-4-ylimino)-methyl]-4-chlorophenol (**HL^4**).* The **HL^4** was prepared by adopting the same procedure as described for **HL^1**, by replacing salicylaldehyde with 5-chloro-2-hydroxybenzaldehyde. On cooling and subsequent slow evaporation, colorless acicular crystals were collected from the mother liquor after 24 h. Yield 88%, mp 230°C, IR spectrum, ν, cm^{-1} 3455 (–OH), 1614 (HC=N), 1302 (C–O), ^{1}H NMR spectrum (DMSO-d_6 400 MHz, δ, ppm): 11.43 s (–OH), 8.31 s (H^1, H$^{1'}$), 10.20 s (HC=N), 6.87 d (H^5, J[^{1}H–^{1}H] = 8.4 Hz), 7.22 d.d (H^6, J[^{1}H–^{1}H] =

8.8, 2.8 Hz), 8.10 d (H^8, $J[^1H–^1H]$ = 2.4 Hz); ^{13}C NMR spectrum (DMSO-d_6 101 MHz, δ, ppm): 137.3 (C^1, $C^{1'}$), 155.1 (C^2), 122.3 (C^3), 177.8 (C^4), 117.6 (C^5), 130.3 (C^6), 123.4 (C^7), 125.4 (C^8), Λ_m (DMSO) 2.3 S cm^2 mol^{-1}.

*e. Synthesis of [VO(saltrz)$_2$] (**1**), [VO(dhtrz)$_2$] (**2**), [VO(ndtrz)$_2$] (**3**), and [VO(cltrz)$_2$] (**4**).* Oxovanadium complexes **1–4** were synthesized by the reaction of vanadyl(V) isopropoxide, [VO(OCHMe$_2$)$_3$], with **HL^1–HL^4** at the ratio 1 : 2 using acetonitrile (MeCN) as a solvent. The green colored complexes **1–4** were precipitated immediately, washed with acetonitrile, and then dried in air.

Complex 1. Yield 85%, mp > 300°C; M_W 441.3. Calculated, %: C 48.99; H 3.20; N 25.39; O 10.88; $C_{18}H_{14}N_8O_3V$. Found, %: C 49.23; H 3.15; N 25.24; O 10.75. IR spectrum, ν, cm^{-1} 1594 (HC=N), 1306 (C–O), 973 (V=O), 554 (V–O), 455 (V–N). μ_{eff}, BM: 2.03, Λ_m (DMSO) 10.1 S cm^2 mol^{-1}.

Complex 2. Yield 79%, mp > 300°C; M_W 473.3. Calculated, %: C 45.68; H 2.98; N 23.68; O 16.90. $C_{18}H_{14}N_8O_5V$. Found, %: C 45.53; H 3.10; N 23.82; O 16.85. IR spectrum, ν, cm^{-1} 1600 (HC=N), 1313 (C–O), 989 (V=O), 570 (V–O), 461 (V–N). μ_{eff}, BM: 1.91, Λ_m (DMSO) 12.9 S cm^2 mol^{-1}.

Complex 3. Yield 86%, mp > 300°C; M_W 541.4, Calculated, %: C 57.68; H 3.35; N 20.70; O 8.87. $C_{26}H_{18}N_8O_3V$. Found, %: C 57.98; H 3.21; N 20.88; O 8.95. IR spectrum, ν, cm^{-1} 1615 (HC=N), 1319 (C–O), 959 (V=O), 562 (V–O), 458 (V–N). μ_{eff}, BM: 1.84, Λ_m (DMSO) 3.4 S cm^2 mol^{-1}.

Complex 4. Yield 93%, mp > 300°C; M_W 510.2. Calculated, %: C 42.38; H 2.37; N 21.96; O 9.41. $C_{18}H_{12}Cl_2N_8O_3V$. Found, %: C 42.45; H 2.35; N 21.85; O 9.35. IR spectrum, ν, cm^{-1} 1604 (HC=N), 1293 (C–O), 960 (V=O), 553 (V–O), 463 (V–N). μ_{eff}, BM: 1.85, Λ_m (DMSO) 2.4 S cm^2 mol^{-1}.

RESULTS AND DISCUSSION

The general method for the synthesis of triazole precursors **HL^1–HL^4** is shown in the scheme (1).

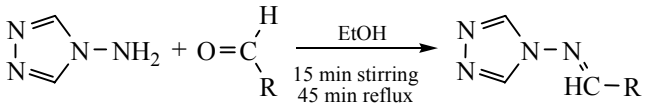

(1)

R = 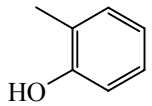 (**HL^1**), 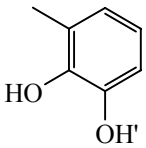 (**HL^2**), 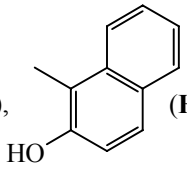 (**HL^3**), 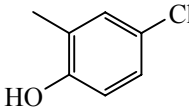 (**HL^4**).

The oxovanadium complexes **1–4** with the synthesized triazole ligands **HL^1–HL^4** were prepared in acetonitrile by the reaction (2).

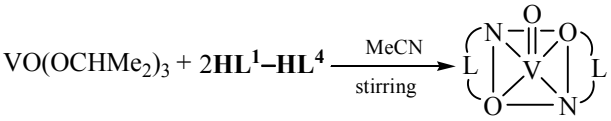

(2)

The spectroscopic and analytical data of the synthesized triazole ligands and their respective oxovanadium complexes are presented in experimental section. The structural formulae of ligands along with the labeling scheme of atoms are shown in Fig. 1.

All synthesized compounds are insoluble in water, whereas the ligands are soluble in organic solvents, like ethanol, methanol, acetonitrile, and chloroform, where DMSO are only soluble among metal complexes. The ligands and their complexes are stable at room temperature in the solid state. The molar conductance of the complexes in DMSO : H_2O (7 : 3) lies between 2.4 to 12.9 S cm^{2}mol^{-1}, indicating their nonelectrolytic nature [21]. The proposed formulae of the compounds were confirmed by the FT-IR, multinuclear (^1H and ^{13}C) NMR, elemental, thermogravimetric, and single crystal analyses.

FT-IR spectroscopy. Triazole Schiff bases showed noticeable peaks in the range from 1602 to 1618 cm^{-1} corresponding to ν(HC=N), which were shifted to

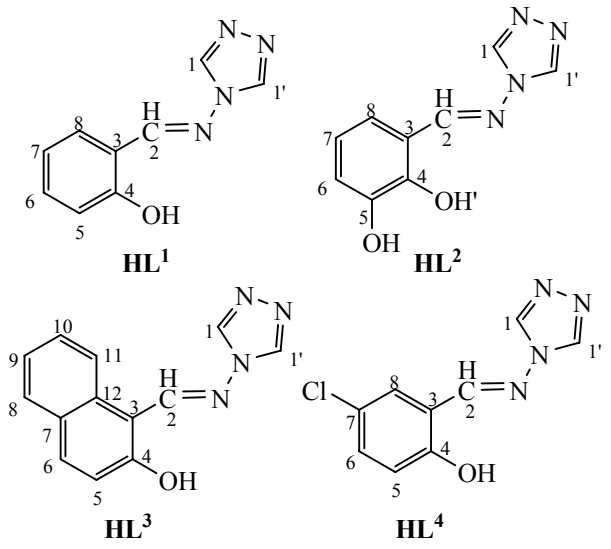

Fig. 1. Scheme of NMR numbering for ligands **HL[1]–HL[4]**.

lower wave numbers, i.e., in the range 1594–1615 cm^{-1} on complexation. The detected shifts of azomethine peaks ν(HC=N) on going from the free triazole Schiff base ligands to the complexes is indicative of bonding of azomethine nitrogen with vanadium atom. In addition, the spectra of the **HL[1]–HL[4]** ligands have broad weak-intensity bands of the ν–OH) vibrations in the range 3435–3455 cm^{-1}, which disappear after chelation, indicating on coordination through the deprotonated form.

This result was further supported by the appearance of two new less intense bands in the range 553–570 and 455–463 cm^{-1}, which are due to ν(V–O) and ν(V–N) vibrations, respectively. Furthermore, the ν(V=O) bands of the medium intensity were also appeared in the region 959-989 cm^{-1}. These results are in agreement with the literature data on these compounds [22, 23]. Based on the perturbation of the azomethine and phenolic group peaks in the FT-IR spectra of the complexes **1–4**, we conclude that the ligands **HL[1]–HL[4]** behave as bidentate.

NMR spectroscopy. The ^{1}H and ^{13}C NMR spectra of the triazole ligands were recorded in deuterated dimethyl sulphoxide (DMSO). The chemical shifts of the protons and carbons agree with the reported values [24, 25] (see experimental section).

The ^{1}H NMR spectra have characteristic peaks of azomethine protons (HC=N) in the range 9.12–10.20 ppm and peaks of hydrogen bonded phenolic protons (–OH) in the range 10.54–11.44 ppm, which confirm the formation of **HL[1]–HL[4]** ligands. In **HL[2]** the non-hydrogen bonded phenolic proton (–OH') gave an upfield signal at 9.25 ppm. Aromatic protons gave signals in the range of 6.73–8.86 ppm. The ^{13}C NMR spectra show characteristic peaks of azomethine carbon (HC=N) in the range 155.1–156.5 ppm, which also supports the formation of **HL[1]–HL[4]** ligands. The signals of carbons in triazole ring appeared in the range 137.3–139.0 ppm, whereas those of the aromatic carbons, in the range 159.4–108.4 ppm. Phenolic carbon in **HL[4]** showed a downfield signal at 177.8 ppm (NMR numbering scheme is given in Fig. 1).

Crystal structures of HL[3] and HL[4]. The data collection and the crystal structure refinement data for ligands **HL[3]** and **HL[4]** are listed in Table 1, together with the standard discrepancy indices, R_1 and wR_2. The selected interatomic parameters for the ligands **HL[3]** and **HL[4]** are listed in Tables 2 and 3, respectively. The ORTEP drawing of the ligands **HL[3]** and **HL[4]** is presented in Figs. 2,3, respectively. The observed bond lengths and bond angles in the ligand precursors are similar to those reported in the literature for other relevant compounds [26]. The XRD data show that **HL[3]** and **HL[4]** are monomers and azomethine nitrogen and phenolic oxygen show hydrogen bonding to form a six-membered ring [27]. For hydrogen bonding, the unsaturated HC=N bond permits π-electronic coupling between the acidic hydrogen and basic nitrogen centers of the molecules. Moreover, this chelate ring is planar in the both Schiff base ligands, which is in accordance with the Ito's et al. data [28]. Ligands **HL[3]** and **HL[4]** showed intramolecular hydrogen bonding as $O–H^{1}\cdots N^{1}$ that stabilizes the molecular conformation. Ligand **HL[3]** is present in the form of a zwitter ion and exhibits intermolecular hydrogen bonding between triazole hydrogen and nitrogen as $C^{12}–H^{12}\cdots N^{3}$ and $C^{13}–H^{13}\cdots N^{4}$. Ligand **HL[4]** shows intermolecular hydrogen bonds of the kind $C^{3}–H^{3}\cdots O^{1}$ and $C^{8}–H^{8}\cdots N^{4}$.

Thermogravimetric study. Thermogravimetric analysis of the complexes **1–4** was carried at temperatures varied from the ambient temperature to 1000°C in the nitrogen atmosphere. The fragments decomposed in the different temperature ranges are listed in Table 4. The table data are in agreement with the results of the elemental analyses and also confirm the composition of the complexes **1–4**. In complexes **1**, **3** and **4,** the vanadium metal, along with some content of organic constituents, is present in the form of residue.

Table 1. Crystal and structure refinement data for **HL**[3] and **HL**[4]

Parameter	Ligand	
	HL[3]	**HL**[4]
Chemical formula	$C_{13}H_{10}N_4O$	$C_9H_7ClN_4O$
Molecular weight	238.25	222.64
T, K	296(2)	296(2)
Wavelength, Å	0.71073	0.71073
Crystal system	Monoclinic	Monoclinic
Space group	$P2_1$	P_C
a, Å	8.7362(3)	3.8468(4)
b, Å	5.8614(2)	14.2942(16)
c, Å	10.9722(4)	9.0339(10)
α, deg	90	90
β, deg	91.874(2)	101.898(4)
γ, deg	90	90
V, Å^3	561.55(3)	486.07(9)
Z	2	2
Absorption coefficient, mm^{-1}	0.095	0.369
F(000)	248	228
Crystal size, mm	0.25×0.18×0.16	0.25×0.14×0.12
θ range for data collection, deg	3.714 to 56.544	2.85 to 54.156
Reflections collected	5600	4027
Independent reflections	2555 (R_{int} = 0.0188)	1841 (R_{int} = 0.0635)
Goodness-of-fit on F^2	1.000	0.0948
Final *R* indices [$I > 2\sigma(I)$]	R_1 = 0.0330, wR_2 = 0.0842	R_1 = 0.0481, wR_2 = 0.0666
R indices (all data)	R_1 = 0.0400, wR_2 = 0.0894	R_1 = 0.1182, wR_2 = 0.0829
Data/restrains/ parameters	2555/1/170	1841/2/137
Density (calculated), mg/m^3	1.409	1.521
CCDC no.	998780	998781

Magnetic moment study. The effective magnetic moment per metal atom was calculated by Eq. (3).

$$\mu_{eff} = 797.5\sqrt{\chi_m T}, \quad (3)$$

where χ_m is the molar magnetic susceptibility of the complex. Diamagnetic correction was made by the use of Pascal's constants for constituent atoms and groups of the complex and as calibrant was used $Hg[Co(SCN)_4]$. The magnetic moments at 298 K for the complexes **1**–**4** were found to be 2.03, 1.91, 1.84, and 1.85 BM, respectively, which confirms their paramagnetic character and the distorted trigonal bipyramidal geometry around the [VO(IV)] ion [29]. These values are characteristic of the monomeric $3d^1$ oxovanadium(IV) complexes with S = 1/2, where metal ion is not involved in the magnetic exchange with the neighboring metal ion or atoms [30].

Table 2. Selected bond lengths (Å), bond angles (deg), and hydrogen bonding in **HL**[3]

Bond length		Bond angle	
O^1–C^1	1.3533	C^1–O^1–H^1	109.00
O^1–H^1	0.9700	N^2–N^1–C^{11}	117.45
N^1–N^2	1.3902	N^1–N^2–C^{12}	132.53
N^1–C^{11}	1.2744	C^{12}–N^2–C^{13}	104.68
N^2–C^{12}	1.3580	N^1–N^2–C^{13}	122.74
N^2–C^{13}	1.3523	N^4–N^3–C^{12}	107.27
N^3–C^{12}	1.2959	N^3–N^4–C^{13}	106.56
N^3–N^4	1.3906	C^{11}–N^1–H^{1A}	118.00
N^4–C^{13}	1.2988	N^2–N^1–H^{1A}	122.00
N^1–H^{1A}	0.7000	C^2–C^1–C^{10}	120.95
C^1–C^{10}	1.3948	N^1–C^{11}– C^{10}	121.38

Hydrogen bonding

D–H···A	*d*[D–H]	*d*[H···A]	*d*[D···A]	[DHA] angle
O^1–H^1···N^1	0.9700	1.7600	2.6037	143.00
C^{12}–H^{12}···N^3	0.9300	2.4300	3.2616	149.00
C^{13}–H^{13}···N^4	0.9300	2.5000	3.2536	138.00

Table 3. Selected bond lengths (Å), bond angles (deg), and hydrogen bonding in **HL**[4]

Bond length		Bond angle	
Cl^1–C^4	1.7475	N^2–N^1–C^7	116.95
O^1–C^1	1.3647	N^1–N^2–C^8	132.85
O^1–H^1	0.8200	N^1–N^2–C^9	122.45
N^1–C^7	1.2888	C^8–N^2–C^9	104.52
N^1–N^2	1.4019	N^4–N^3–C^8	107.00
N^2–C^8	1.3536	N^3–N^4–C^9	107.10
N^2–C^9	1.3623	O^1–C^1–C^6	122.49
N^3–C^8	1.2980	O^1–C^1–C^2	117.01
N^3–N^4	1.3883	Cl^1–C^4–C^5	118.92
N^4–C^9	1.2923	N^2–C^8–N^3	110.72

Hydrogen bonding

D–H···A	*d*[D–H]	*d*[D···A]	[DHA] angle
O^1–H^1···N^1	0.8200	2.6285	145.00
C^3–H^3···O^1	0.9300	3.4162	164.00
C^8–H^8···N^4	0.9300	3.2589	170.00

Electronic absorption titration. The interaction of triazole ligands and their oxovanadium complexes with SS-DNA was studied by the UV absorption spectroscopy**.** Generally, DNA binding occurs in three different modes: (1) Electrostatic interaction with the negatively charged nucleic sugar-phosphate structure, which is along the external DNA double helix and do not possess selectivity (2) binding interaction with grooves of the DNA double helix, and (3) intercalation between the stacked base pairs of native DNA [31].

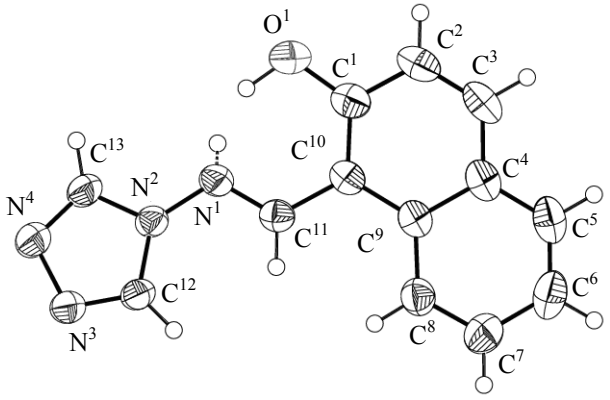

Fig. 2. The ORTEP drawing of the ligand **HL**[3] with the displacement ellipsoids at the 50% probability level.

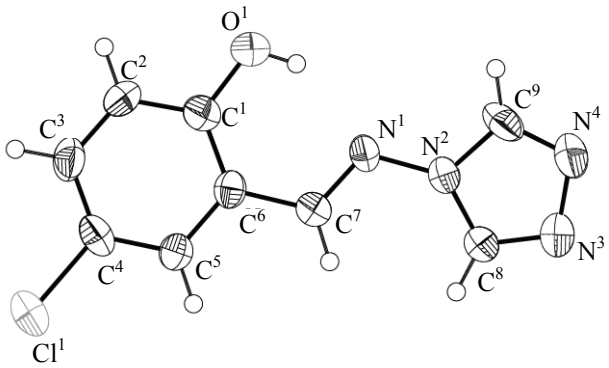

Fig. 3. The ORTEP drawing of the ligand **HL**[4] with the displacement ellipsoids at the 50% probability level.

Table 4. Thermogravimetric data on the oxovanadium complexes **1–4**

Complex no.	Temperature, °C	Evolved components	Weight loss, %	
			experimental	calculated
1	53–238	N_2	6.17	6.35
	238–362	$C_3H_3N_2$	15.77	15.20
	362–431	$C_3H_3N_4$	22.36	21.54
	431–948	C_9H_7	24.72	26.09
	>948	Residue (C_3HO_3V)	30.92	30.82
2	44–230	2OH	7.22	7.18
	230–261	$2C_2H_2N_4$	35.08	34.67
	261–951	$C_{14}H_8O_3V$	56.53	58.13
	951	Residue	1.01	0.02
3	50–236	N_2CH	7.44	7.58
	236–285	$C_3H_3N_3$	14.76	14.97
	285–458	$C_6H_6N_3$	22.47	22.19
	458–717	C_5H_4	11.85	11.84
	717–951	C_8H_3	17.75	18.30
	>951	Residue (C_3HO_3V)	25.68	25.12
4	37–217	$C_2H_2N_2$	10.51	10.59
	217–284	$C_3H_3N_4$	18.13	18.63
	284–502	$C_7H_4ClN_2$	29.61	29.71
	502–951	C_5H_3Cl	19.61	19.31
	>951	Residue (CO_3V)	22.01	21.76

Hyperchromic and hypochromic effects are the spectral features of DNA concerning its double helix structure. The hypochromism results from the contraction of DNA in the helix axis, as well as from the change in conformation on DNA, while the hyperchromism results from the damage of the DNA double helix structure [32]. The absorption spectra of the metal complex bound to DNA through the intercalation exhibit the hypochromism and show a red/blue shift due to the strong π–π* stacking interaction between the aromatic chromophore of the metal complexes and the base pairs of DNA.

The UV-visible titrations of the ligands **HL[1]–HL[4]** and oxovanadium complexes **1**, **3,** and **4,** in the absence (*1*) and in the presence (*2–10*) of SS-DNA have been studied in tris buffer solution in the wavelength range 600–250 nm at a constant concentration of the complexes. Two representative absorption spectra of **HL[3]** and complex **3** are shown in Fig. 4. After 24 h, the spectra were the same, i.e., the drug-DNA adduct is stable. The data obtained were substituted into the following Benesi–Hildebrand relationship [33] to determine the intrinsic binding constant K from Eq. (4):

$$\frac{A_0}{A - A_0} - \frac{\varepsilon_G}{\varepsilon_{H-G} - \varepsilon_G} + \frac{\varepsilon_G}{\varepsilon_{H-G} - \varepsilon_G} \frac{1}{K[DNA]}, \quad (4)$$

where K is the binding constant, A_0 and A is the absorbance of drug and drug-SS-DNA adduct, respectively, and ε_G, ε_{H-G} is the absorption coefficient of drug and drug-SS-DNA adduct, respectively.

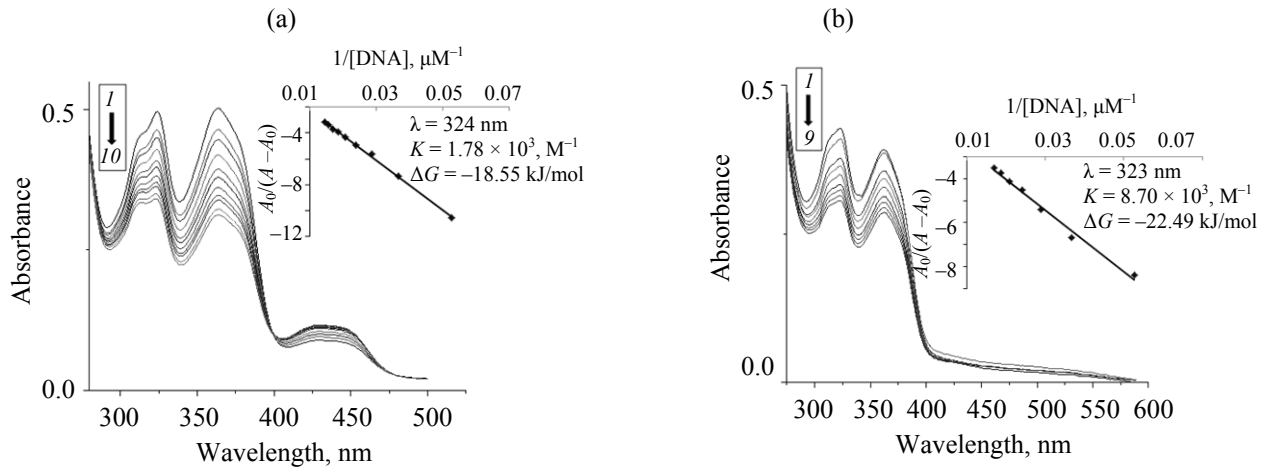

Fig. 4. Absorption spectra of the ligand (a) **HL**[3] and (b) its oxovanadium complex **3** in the (a) absence and (b) in the presence of DNA. DNA concentration (μM): (*1*) 10, (*2*) 19, (*3*) 27, (*4*) 35, (*5*) 42, (*6*) 48, (*7*) 54, (*8*) 59, (*9*) 64, and (*10*) 68. The arrow indicates increasing DNA concentrations. The insert is the $A_0/(A - A_0)$ vs 1/[DNA] plot.

The binding constants were obtained from the $A_0/(A - A_0)$ vs. 1/[DNA] plots. The change in the Gibb's free energy (ΔG) was determined from Eq. (5):

$$\Delta G = -RT\ln K, \quad (5)$$

where R is the general gas constant (8.314 J K^{-1} mol^{-1}), T, temperature (K), and K, binding constant.

Complex **2** did not interact with SS-DNA and therefore is not discussed further. The determined values of the absorption bands' maxima, λ_{max}, their shifts, binding constants (K), and the Gibb's free energy (ΔG) are listed in Table 5. These spectral characteristics showed hypochromism and a blue shift with the increase in the DNA concentration for **HL**[2]**–HL**[4] and for complexes **1**, **3,** and **4**. These compounds may interact with DNA by the intercalation and groove binding mechanisms. After intercalating with the base pairs of DNA, the π* orbital of the intercalated ligand could be coupled with the π orbital of the base pairs, thus decreasing the π–π* transition energy. It also shows a minor interaction with the grooves through hydrogen bonding with bases, typically to N^3 of adenine and O^2 of thymine [34]. These findings are in agreement with the reported studies on oxovanadium complexes [35, 36]. On the other hand, the hypochromism with a red shift exhibited by **HL**[1] shows that the drug-DNA interaction occurs by the electrostatic and groove binding mechanisms.

The determined binding constants of complexes **3** (8.7×10^3) and **4** (6.32×10^3) were higher than those of their free ligands. This might be due to the presence of oxovanadium moiety, which assists the stacking interaction with DNA. However, the binding of **HL**[1] with DNA occurs via the electrostatic interaction, as mentioned above.

Table 5. Data on the Drug-DNA interaction

Compound	λ_{max}, nm	Hypochromism, %	Bathochromism, nm	Hypsochromism, nm	$K \times 10^3$, M^{-1}	ΔG, kJ/mol
HL[1]	330	23.18	1	–	4.18± 0.91	–20.66± 0.55
1	329	20.09	–	4	3.03± 0.09	–19.86± 0.36
HL[2]	292	27.25	–	2	9.64± 1.14	–22.72± 0.30
HL[3]	324	31.15	–	2	1.78± 0.43	–18.55± 0.61
3	323	28.50	–	1	8.70± 0.99	–22.49± 0.29
HL[4]	342	29.30	–	2	1.00± 0.43	–17.11± 1.16
4	341	25.71	–	2	6.32± 0.95	–21.60± 0.38

The Gibb's free energy of the ligands $\mathbf{HL^1}$–$\mathbf{HL^4}$ and complexes **1**, **3** and **4** lie from –6.9 to –20.6 and from –15.93 to –22.48 kJ/mol, respectively, which shows that the drug-DNA interaction is the spontaneous process.

Enzyme inhibition study. The *v*anadate ion is a potent competitive inhibitor of phosphatase because it is isostructural and isoelectronic to phosphate [37, 38]. Like the phosphate ion, it can form stable five-coordinated species, and therefore, may serve as a transition-state analog for both the acquisition of phosphate and its release in the catalytic reaction of alkaline phosphatase [39]. The ALP hydrolysis of *p*-NPP occurs by Eq. (6) to form a yellow-colored *p*-nitrophenol that absorbs at 405 nm.

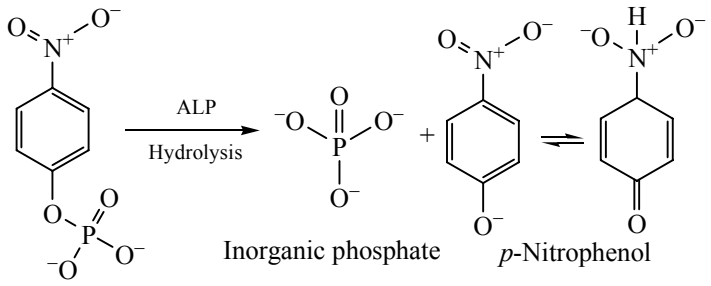

(6)

The activity of the enzymes decreases, as the concentration of the compound increases. The X-ray crystal structure of Yersinia PTP (protein-tyrosine phosphatase) complexed with vanadate suggests that the vanadate occupies the active site of the phosphatase enzyme to form a thiol-vanadyl ester linkage with a catalytic cysteine residue [40]. All the synthesized triazole precursors ($\mathbf{HL^1}$–$\mathbf{HL^4}$) and the oxovanadium complexes **1–4** were screened for their inhibition against ALP. The results are shown in Fig. 5. All the triazole precursors tested are inactive against ALP inhibition, while their oxovanadium complexes exhibit activity, depending on concentration. Among the tested series, the complex **4** is the most potent inhibitor since it completely inhibits the ALP at the concentration of 184 mM and above. It was also found that at a concentration of 0.247 mM the ALP inhibition is 100% for all complexes. These findings agree with the fact that the vanadium compounds inhibit over 50% of ALP activity at concentrations above 50 μM [41]. Probably, the quantitative inhibition of ALP by the tested compounds could be due to their binding with the active sites of ALP, which results in the failure of the enzyme and catalyses the reaction. Consequently, the absorption decrease is due to the formation of a lesser amount of the product.

Antimicrobial activities. The synthesized free ligands and their respective oxovanadium complexes were screened to see their in vitro response against various strains of fungi (*Alternaria alternata*, *Ganoderma lucidum*, *Aspergillus niger* and *Penicillium notatum*) and bacteria (*Escherichia coli*, *Bacillus subtilis*, *Staphylococcus aureus* and *Pasturella multocida*) by disc diffusion method. Fluconazole and Streptomycin were used as positive controls for antifungal and antibacterial screening tests, respectively, whereas DMSO was used as negative control. Each disc (9 mm) was soaked with a sample solution (1 mg/mL of drug in DMSO) [42] and the zones of inhibition formed in the respective media were measured in millimeters. Percentage of growth inhibition was calculated with reference to the growth in a control from Eq. (7).

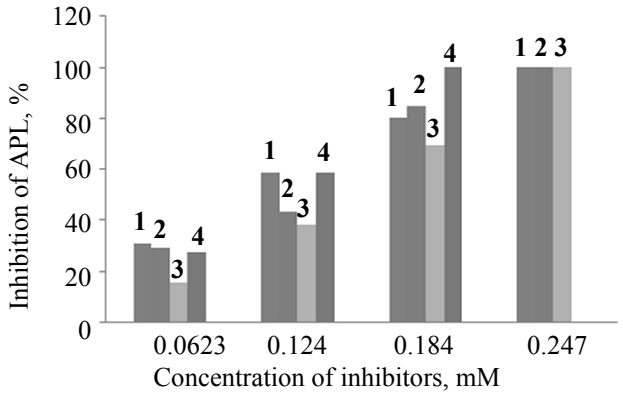

Fig. 5. Inhibition of alkaline phosphatase (ALP) with the oxovanadium complexes **1–4**.

$$\text{Growth inhibition, \%} = 100 - \left(\frac{\text{Linear growth in test sample, nm}}{\text{Linear growth in control, nm}} \times 100 \right). \quad (7)$$

The data obtained are summarized in Tables 6 and 7. It was found that, in general, the vanadium complexes have significantly higher activity towards all the tested organisms than the respective free ligand precursors. Among all thetriazol ligands, the activity of **HL**^{3} and **HL**^{4} against all fungal species was maximal; the antifungal activity of their complexes was also maximal, as compared to all novel complexes studied, and even exceeded that of the standard control drug.

The greater antifungal activity of the tested triazol ligands and their oxovanadium complexes was accounted

Table 6. Antifungal activity of the ligands **HL**^{1}**–HL**^{4} and their oxovanadium complexes **1–4**

Compound	Average zone of inhibition, mm			
	A. alternata	*G. lucidum*	*A. niger*	*P. notatum*
Fluconazole	$38.33^{a,b} \pm 0.41$	$41.29^{a,b} \pm 0.51$	$40.33^{a,b} \pm 0.36$	$35.44^{b,c} \pm 0.27$
HL^{1}	$20.11^{c} \pm 0.10$	$18.15^{c} \pm 0.12$	$25.08^{c} \pm 0.14$	$22.18^{c} \pm 0.17$
1	$25.20^{b,c} \pm 0.18$	$23.33^{b,c} \pm 0.17$	$33.25^{b,c} \pm 0.20$	$27.21^{b,c} \pm 0.14$
HL^{2}	$29.12^{b,c} \pm 0.19$	$23.29^{b,c} \pm 0.14$	$26.21^{b,c} \pm 0.12$	$25.29^{b,c} \pm 0.15$
2	$34.04^{a,b} \pm 0.07$	$34.26^{b,c} \pm 0.18$	$31.71^{b,c} \pm 0.15$	$37.16^{b,c} \pm 0.28$
HL^{3}	$30.25^{b,c} \pm 0.22$	$41.37^{a,b} \pm 0.21$	$35.39^{b,c} \pm 0.27$	$55.37^{a,b} \pm 0.33$
3	$39.66^{a,b} \pm 0.28$	$56.33^{a} \pm 0.14$	$47.29^{a,b} \pm 0.28$	$62.37^{a} \pm 0.43$
HL^{4}	$32.24^{a,b} \pm 0.16$	$34.71^{b,c} \pm 0.15$	$32.21^{b,c} \pm 0.14$	$35.29^{b,c} \pm 0.19$
4	$42.19^{a} \pm 0.17$	$52.25^{a,b} \pm 0.12$	$52.36^{a} \pm 0.13$	$60.31^{a,b} \pm 0.18$

Concentration is 1 mg/mL in DMSO; 0 = No activity, 5–10 = Activity is present, 11–25 = Moderate activity, 26–40 = Strong activity; Antibacterial values are the average values obtained in three independent measurements at $p < 0.1$; Letters in superscripts denote activity level: ^{a} maximum, ^{b} intermediate, ^{c} minimum, ^{a,b} between maximum and intermediate, and ^{b,c} between intermediate and minimum; the same for Table 7.

Table 7. Antibacterial activity of the ligands **HL**^{1}**–HL**^{4} and their oxovanadium complexes **1–4**

Compound	Average zone of inhibition (mm)			
	E. coli	*B. subtilis*	*S. aureus*	*P. multocida*
Streptomycin	$30.33^{a,b} \pm 0.26$	$30.29^{a} \pm 0.19$	$30.37^{a} \pm 0.33$	$30.29^{a,b} \pm 0.29$
HL^{1}	$20.37^{c} \pm 0.14$	$19.29^{c} \pm 0.15$	$18.21^{c} \pm 0.14$	$21.33^{c} \pm 0.14$
1	$26.32^{b,c} \pm 0.20$	$25.23^{a,b} \pm 0.12$	$23.12^{b} \pm 0.19$	$23.33^{b,c} \pm 0.26$
HL^{2}	$22.17^{b,c} \pm 0.13$	$22.09^{b,c} \pm 0.18$	$20.08^{b,c} \pm 0.14$	$22.13^{b,c} \pm 0.20$
2	$30.33^{a,b} \pm 0.26$	$25.17^{a,b} \pm 0.23$	$27.15^{a,b} \pm 0.23$	$25.16^{b,c} \pm 0.07$
HL^{3}	$28.46^{a,b} \pm 0.18$	$27.25^{a,b} \pm 0.12$	$27.37^{c} \pm 0.21$	$26.28^{a,b} \pm 0.16$
3	$35.31^{a} \pm 0.27$	$30.42^{a} \pm 0.11$	$28.46^{b,c} \pm 0.10$	$29.87^{a,b} \pm 0.21$
HL^{4}	$28.66^{a,b} \pm 0.31$	$24.29^{b,c} \pm 0.15$	$25.23^{b} \pm 0.09$	$25.14^{b,c} \pm 0.17$
4	$34.27^{a,b} \pm 0.18$	$29.21^{a,b} \pm 0.14$	$29.25^{a,b} \pm 0.22$	$30.75^{a} \pm 0.13$

for by the fact that their structure is bulky and has electronegative nature, which results in a larger lipophilicity and assists diffusion through the microbial cell membrane and, consequently, ensures larger microbial sensitivity towards these drugs. It was also found that oxovanadium complexes are more active inhibitors against fungal culture than bacterial growth, which is in accordance with the literature data [42].

Hemolytic activity. The hemolytic activity was studied, because the compound having antimicrobial activity cannot be used in medicine, if its hemolytic properties are unknown [42].

The hemolytic bioassays of the synthesized complexes were performed with human red blood cells in vitro with respect to the Triton X-100 and PBS as positive control (100% lysis) and negative control (0% lysis), respectively. The percentage of hemolysis was calculated by Eq. (8) [43]:

$$\text{Hemolysis, \%} = \frac{\text{Abs}_{\text{sample}}}{\text{Abs}_{\text{control}}} \times 100. \quad (8)$$

The values of the hemolytic activity are listed in Table 8, as the average of three independent measurements. As seen, the activity of all complexes synthesized here is significantly lower than that of TrilonX-100 and higher than that of PBS. The activity of complexes **2** and **3** is increased in comparison with the corresponding ligands $\mathbf{HL^2}$ and $\mathbf{HL^3}$, whereas the activity of the vanadium complexes **1** and **4** is decreased compared to the non-coordinated free ligands $\mathbf{HL^1}$ and $\mathbf{HL^4}$. The compounds showing higher activity may be used for further study on antitumor activity.

Insulin mimetic study. Potential antidiabetic activity of triazole precursors $\mathbf{HL^1}$–$\mathbf{HL^4}$ and their oxovanadium complexes **1**–**4** was tested on BALB/c albino mice. In general, the animals retained health and activity. Positive control was treated with Glibenclamide and negative control, with Alloxan only (see Figs. 6, 7). The results obtained are in agreement with the published data on other oxovanadium(IV) complexes [44, 45].

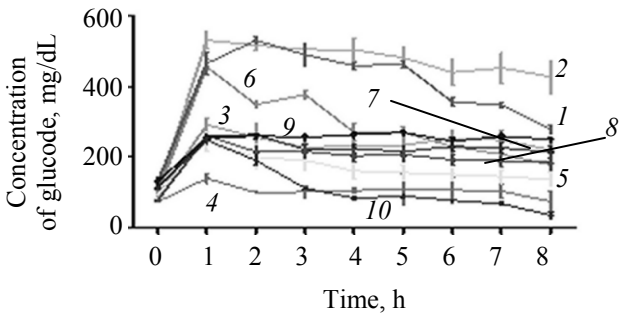

Fig. 6. Concentration of plasma glucose in mice treated with the synthesized ligands ($\mathbf{HL^1}$–$\mathbf{HL^4}$) and their oxovanadium complexes **1**–**4**. Negative control was treated with Alloxan, whereas positive control was treated with Glibenclamide. (*) $p < 0.001$, $q = 4.4$. (*1*) Negative control, (*2*) positive control, (*3*) $\mathbf{HL^1}$, (*4*) complex **1**, (*5*) $\mathbf{HL^2}$, (*6*) complex **2**, (*7*) $\mathbf{HL^3}$, (*8*) complex **3**, (*9*) $\mathbf{HL^4}$, (*10*) complex **4**.

The ligand $\mathbf{HL^1}$ showed a significant glucose-lowering potential, as compared with the negative control, whereas in comparison with the positive control, no glucose lowering was observed ($p < 0.001$; Fig. 6). This compound led to a significant decrease in the cholesterol concentration ($p < 0.001$; Fig. 7a), whereas caused a significant increase in the total serum triglycerides' concentration ($p < 0.001$; Fig. 7b). The treatment with the complex **1** led to a significant lowering of a plasma glucose, as compared to negative control ($p < 0.001$; Fig. 6). The cholesterol concentration considerably decreased in comparison with negative control, whereas the concentration of serum triglyceride increased significantly in comparison with positive and negative controls ($q = 4.450$; Fig. 7a) and ($p < 0.001$; Fig. 7b).

The ligand $\mathbf{HL^2}$ caused a significant reduction in the plasma glucose concentration against negative control ($p < 0.001$; Fig. 6), whereas to an increase in the concentration of serum cholesterol ($p < 0.019$; Fig. 7a). However, for triglyceride, effect was insignificant (Fig. 7b). Complex **2** significantly reduced the the plasma glucose (Fig. 6) and serum cholesterol ($q = 4.550$; Fig. 7a) concentrations. In contrast, it did not affect the concentration of serum triglyceride (Fig. 7b).

Table 8. Hemolytic activity of the ligands $\mathbf{HL^1}$–$\mathbf{HL^4}$ and their oxovanadium complexes **1**–**4**

Compound	$\mathbf{HL^1}$	**1**	$\mathbf{HL^2}$	**2**	$\mathbf{HL^3}$	**3**	$\mathbf{HL^4}$	**4**	Triton-X 100
Hemolysis, %	72.41±0.02	62.24±0.03	41.15±0.05	55.31±0.02	32.79±0.03	42.21±0.04	49.32±0.06	25.12±0.01	99.53±0.72

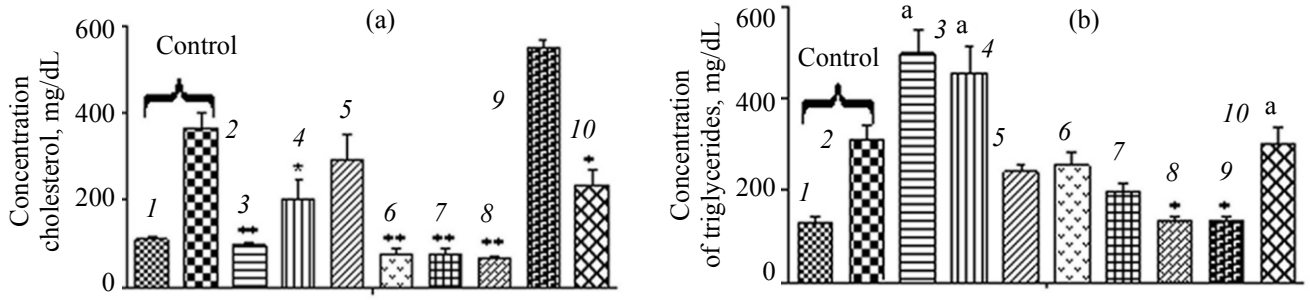

Fig. 7. Concentration of serum cholesterol (a) and triglycerides (b) in mice treated with the ligands $\mathbf{HL^1}$-$\mathbf{HL^4}$ and their oxovanadium complexes **1-4**. Negative control was treated with Alloxan only and positive control, with Glibenclamide. (*) $p < 0.001$, $q = 4.40$. (a) $p < 0.001$. (*1*) Negative control, (*2*) positive control, (*3*) $\mathbf{HL^1}$, (*4*) complex **1**, (*5*) $\mathbf{HL^2}$, (*6*) complex **2**, (*7*) $\mathbf{HL^3}$, (*8*) complex **3**, (*9*) $\mathbf{HL^4}$, (*10*) complex **4**.

In the presence of the ligand $\mathbf{HL^3}$, the concentrations of plasma glucose ($p < 0.015$; Fig. 6) and serum cholesterol ($q = 4.550$; Fig. 7a) reduced significantly, whereas the concentration of serum triglyceride did not change (Fig. 7b). Administration of the complex **3** led to a significant lowering of plasma glucose, serum cholesterol, and triglyceride concentrations (Figs. 6, 7a, and 7b).

The treatment with the ligand $\mathbf{HL^4}$ did not decrease the plasma glucose and cholesterol concentrations, whereas reduced the triglyceride concentration ($q = 4.400$; $p < 0.05$, Figs. 6, 7a, and 7b). The complex **4** led to a significant reduction of the plasma glucose concentration, but caused the increase in the concentrations of serum cholesterol and triglyceride ($p < 0.019$; $p < 0.05$, Figs. 6, 7a, and 7b).

CONCLUSIONS

In the study, triazole Schiff bases and their respective oxovanadium(IV) complexes were synthesized and their properties were determined by the elemental analysis, FT-IR, NMR, spectroscopies, thermogravimetry, magnetic moment method, conductometry, and X-ray crystallography. The study showed that the complexation of ligands with the vanadium ion occurs through the azomethine nitrogen and phenolic oxygen of the precursors. The ligand, being complexed acts as monobasic, bidentate ligand. The data on the UV-Vis spectroscopy show that the binding of the synthesized compounds with SS-DNA occurs by the intercalation, electrostatic, and groove binding mechanisms. The improved biological activities of the azomethine linkage or heteroaromatic nuclei during the complexation may be due to the increased hydrophobic character and lipo-solubility of the molecules. The d^1 electronic configuration of vanadium in the vanadium complexes was confirmed. The synthesized compounds exhibit excellent antidiabetic properties.

Crystallographic data for the reported structures are deposited with the Cambridge Crystallographic Data Centre, CCDC (998780 and 998781 for $\mathbf{HL^3}$ and $\mathbf{HL^4}$, respectively).

ACKNOWLEDGMENTS

K.S. Munawar is thankful to the Higher Education Commission, Islamabad, Pakistan, for the financial support of this study.

REFERENCES

1. Koo, B.K., Jang, Y.J., and Lee, U., *Bull. Korean Chem. Soc.,* 2003, vol. 24, p. 1014.
2. Maurya, M.R., Kumar, A., Bhat, A.R., Azam, A., Bader, C., and Rehder, D., *Inorg. Chem.,* 2006, vol. 45, p. 1260.
3. Frank, P., Carlson, R.M.K., Carlson, E.J., and Hodgson, K.O., *Coord. Chem. Rev.,* 2003, vol. 237, p. 31.
4. Berry, R.E., Armstrong, E.M., Beddoes, R.L., Collison, D., Ertok, S.N., Helliwell, M., and Garner, C.D., *Angew. Chem. Int. Edit*., 1999, vol. 38, p. 795.
5. Thompson, K.H., Lichter, J., LeBel, C., Scaife, M.C., McNeil, J.H., and Orvig, C., *J. Inorg. Biochem.,* 2009, vol. 103, p. 554.
6. Srivastava, A.K. and Mehdi, M.Z., *Diabetic Med.,* 2005, vol. 22, p. 2.
7. Hiromura, M., Nakayama, A., Adachi, Y., Doi, M., and Sakurai, H., *J. Biol. Inorg. Chem.,* 2007, vol. 12, p. 1275.
8. McNeil, J.H., Yuen, V.G., Hoveyda, H.R., and Orvig, C., *J. Med. Chem.*, 1992, vol. 35, p. 1489.
9. Venkataraman, B.V. and Sudha, S., *Asian J. Exp. Sci.*, 2005, vol. 19, p. 127.

10. Haasnoot, J.G., *Coord. Chem. Rev.*, 2000, vol. 200, p. 131.
11. Aromi, G., Barrios, L.A., Roubeau, O., and Gamez, P., *Coord. Chem. Rev.*, 2011, vol. 255, p. 485.
12. Sheldrick, G.M., *Acta Crystallogr. A.*, 2008, vol. 64, p. 112.
13. Dey, S., Sarkar, S., Paul, H., Zangrando, E., and Chattopadhyay, P., *Polyhedron,* 2010, vol. 29, p. 1583.
14. Sastri, C.V., Eswaramoorthy, D., Giribabu, L., and Maiya, B.G., *J. Inorg. Biochem.,* 2003, vol. 94, p. 138.
15. Malik, M.R., Vasylyeva, V., Merz, K., Metzler-Nolte, N., Saleem, M., Ali, S., Isab, A.A., Munawar, K.S., and Ahmad, S., *Inorg. Chim. Acta*, 2011, vol. 376, p. 207.
16. Jabeen, M., Ali, S., Shahzadi, S., Shahid, M., Khan, Q.M., Sharma, S.K., and Qanungo, K., *J. Iran. Chem. Soc.*, 2012, vol. 9, p. 307.
17. National Committee for Clinical Laboratory Standards. *Performance Standards for Antimicrobial Disc Susceptibility Test,* 5th ed., Approved Standard, M2-A6; Clinical and Laboratory Standards Institute: Wayne, PA, USA, 1997.
18. Bhalodia, N.R. and Shukla, V.J., *J. Adv. Pharm. Technol. Res.,* 2011, vol. **2**, p. 104.
19. Huynh, Q.K., Borgmeyer, J.R., Smith, C.E., Bell, L.D., and Shah, D.M., *J. Biol. Chem.,* 2001, vol. 316, p. 723.
20. Iqbal, Z., Ali, S., Iqbal, J., Abbas, Q., Qureshi, I.Z., and Hameed, S., *Bioorg. Med. Chem. Lett*., 2013, vol. 23, p. 488.
21. Chohan, Z.H., Sumrra, S.H., Youssoufi, M.H., and Hadda, T.B., *Eur. J. Med. Chem.,* 2010, vol. 45, p. 2739.
22. Lalami, N.A., Monfared, H.H., Noei, H., and Mayer, P., *Transit. Metal. Chem.,* 2011, vol. 36, p. 669.
23. Agarwal, R.K., Singh, L., Sharma, D.K., and Singh, R., *Turk. J. Chem.,* 2005, vol. 29, p. 309.
24. Mohammadi, K. and Rastegari, M., *Spectrochim. Acta A,* 2012, vol. 97, p. 711.
25. Rayati, S., and Ashouri, F., *C. R. Chim.,* 2012, vol. 15, p. 679.
26. Sharma, P., and Sharma, J.D., *J. Ethnopharmacol.,* 2001, vol. 74, p. 239.
27. Munawar, K.S., Ali, S., and Tahir, M.N., *Acta Cryst. E.,* 2011, vol. 67, p. o77.
28. Ito, E., Oji, H., Araki, T., Oichi, K., Ishii, H., Ouchi, Y., Ohta, T., Kosugi, N., Maruyama, Y., Naito, T., Inabe, T., and Seki, K., *J. Am. Chem. Soc.,* 1997, vol. 119, p. 6336.
29. Maurya, R.C. and Rajput, S., *J. Mol. Struct.*, 2004, vol. 687, p. 35.
30. Patel, M.N., Patel, S.H., Chhasatia, M.R., and Desai, C.R., *Nucleos. Nucleot. Nucl.* 2010, vol. 29, p. 200.
31. Zhou, C.Y., Zhao, J., Wu, Y.B., Yin, C.X., and Yang, P., *J. Inorg. Biochem.,* 2007, vol. 101, p. 10.
32. Li, Q.S., Yang, P., Wang, H.F., and Guo, M.L., *J. Inorg. Biochem.,* 1996, vol. 64, p. 181.
33. Shuja, S., Shah, A., Rehman, Z., Muhammad, N., Ali, S., Qureshi, R., Khalid, N., and Meetsma, A., *Eur. J. Med. Chem.,* 2010, vol. 45, p. 2902.
34. Haq, I., *Arch. Biochem. Biophys.,*2002, vol. 403, p. 1.
35. Jing, B., Dong, J., Li, J., Xu, T., and Li, L., *J. Coord. Chem.,* 2013, vol. 66, p. 520.
36. Liao, X.W., Lu, J.Z., Ying, P., Zhao, P., Bai, Y.L., Li, W.J., and Liu, M.P., *J. Biol. Inorg. Chem.,* 2013, vol. 18, p. 975.
37. Seargeant, L.E., and Stinson, R.A., *Biochem. J.,* 1979, vol. 181, p. 247.
38. Meng, T.C., Buckley, D.A., Galic, S., Tiganis, T., and Tonks, N.K., *J. Biol. Chem.*, 2004, vol. 279, p. 37716.
39. Holtz, K.M., Stec, B., and Kantrowitz, E.R., *J. Biol. Chem.,* 1999, vol. 274, p. 8351.
40. Huyer, G., Liu, S., Kelly, J., Moffat, J., Payette, P., Kennedy, B., Tsaprailis, G., Gresser, M.J., and Ramachandran, C., *J. Biol. Chem.,* 1997, vol. 272, p. 843.
41. Barrio, D.A., Braziunas, M.D., Etcheverry, S.B., and Cortizo, A.M., *Trace Elements Med. Biol.,* 1997, vol. 11, p. 110.
42. Hussain, S., Bukhari, I.H., Ali, S., Shahzadi, S., Shahid, M., and Munawar, K.S., *J. Coord. Chem.*, 2015, vol. 68, p. 662.
43. Unver, H., Yildiz, M., Ozbay, H., Durlu, T.N., *Spectrochim. Acta,* 2009, vol. 74, p. 1095.
44. Crans, D.C., Smee, J.J., Gaidamauskas, E., and Yang, L., *Chem. Rev.,* 2004, vol. 104, p. 849.
45. Sheela, S., Roopan, S.M., and Vijayaraghavan, R., *Eur. J. Med. Chem.*, 2008, vol. 43, p. 2206.